STUDIES ON CODING TECHNIQUES AND IT'S APPLICATION TO OTDR

A Project Report
Submitted in partial fulfilment of the requirements for the award of the degree
Of

BACHELOR OF TECHNOLOGY
IN
ELECTRONICS AND COMMUNICATION ENGINEERING

By

Sudharani Kindo (10509008)
V Jaikishen (10509011)
Under the guidance of
Prof. P.K. Sahu

Department of Electronics & Communication Engineering
National Institute of Technology
Rourkela,769008 (2008-2009)

STUDIES ON CODING TECHNIQUES AND IT'S APPLICATION TO OTDR

A Project Report
Submitted in partial fulfilment of the requirements for the award of the degree
Of

BACHELOR OF TECHNOLOGY
IN
ELECTRONICS AND COMMUNICATION ENGINEERING

By
Sudharani Kindo (10509008)
V Jaikishen (10509011)
Under the guidance of
Prof. P.K. Sahu

Department of Electronics & Communication Engineering
National Institute of Technology
Rourkela, 769008 (2008-2009)

National Institute of Technology
Rourkela

CERTIFICATE

This is to certify that the thesis entitled, "Studies on coding techniques and its application to OTDR" submitted by Sudharani Kindo in partial fulfillments for the requirements for the award of Bachelor of Technology Degree in Electronics & Communication Engineering at National Institute of Technology, Rourkela (Deemed University) is an authentic work carried out by her under my supervision and guidance.

To the best of my knowledge, the matter embodied in the thesis has not been submitted to any other University / Institute for the award of any Degree or Diploma.

Date:

Prof. P. K. SAHU
Dept. of Electronics & Communication Engg.
National Institute of Technology
Rourkela - 769008

ACKNOWLEDGEMENT

We place on record and warmly acknowledge the continuous encouragement, invaluable supervision, timely suggestions and inspired guidance offered by our guide ***Prof. P.K.Sahu,*** *Professor, Department of Electronics and Communication Engineering, National Institute of Technology, Rourkela, in bringing this report to a successful completion.*

We are grateful to ***Prof. S.K.Patra****, Head of the Department of Electronics and communication Engineering, for permitting us to make use of the facilities available in the department to carry out the project successfully. Last but not the least we express our sincere thanks to all of our friends who have patiently extended all sorts of help for accomplishing this undertaking.*

We are particularly grateful to ***Prof S.K. Varshney****, Professor, Department of Electrical and Electronics Communication Engineering, Indian Institute of Technology, Kharagpur and* ***Mr. Utpal Patra****, in charge of Optics Lab at the same for permitting us to use the resources available there to carry out the project successfully.*

Finally we extend our gratefulness to one and all who are directly or indirectly involved in the successful completion of this project work.

V Jaikishen (10509011)
Sudharani Kindo (10509008)

Abstract:

In the following thesis, we will be discussing the different aspects and parameters involving Optical Time Domain Reflectometer (OTDR) as well as different aspects of unipolar coding techniques. The purpose of this thesis is to fully understand the methods by which unipolar codes like the Golay and Simplex codes are created from Hadamard matrices and to understand its application in Optical Time Domain Reflectometry. Furthermore, this thesis also delves into the region of performance enhancement of Optical Time Domain Reflectometer by means of implementation of these coding techniques.

Contents

List of Figures:

List of tables:

CHAPTER 1

BASICS OF AN OPTICAL TIME DOMAIN REFLECTOMETER.

1.1 Introduction to OTDR:

OTDR (Optical Time-Domain Reflectometer) is a device that is used to determine the nature and location of faults in optical fibers. In order to determine faults, the OTDR sends a pulse into the fiber and records the reflected light and plots a response graph. When light is sent through a glass fiber link, some of the light is reflected back to the transmitter (this is known as backscattering). When characterizing a fiber link using an OTDR, it is this reflected light that is used to calculate the attenuation of the link, the characteristics of loss and the length of the fibre span. The OTDR software displays the faults and fibre joints on a generated graph that is called trace. Faults and Connections can be determined from display of the OTDR.

A typical OTDR trace is shown in figure 1. As we can see from the figure, there is a table on the display below the trace. This table lists all the faults in the fibre in the form of events, namely connectors, splices, fibre breaks etc. A good quality OTDR should be able to determine faults and display them in such a manner that it is understood by the user.

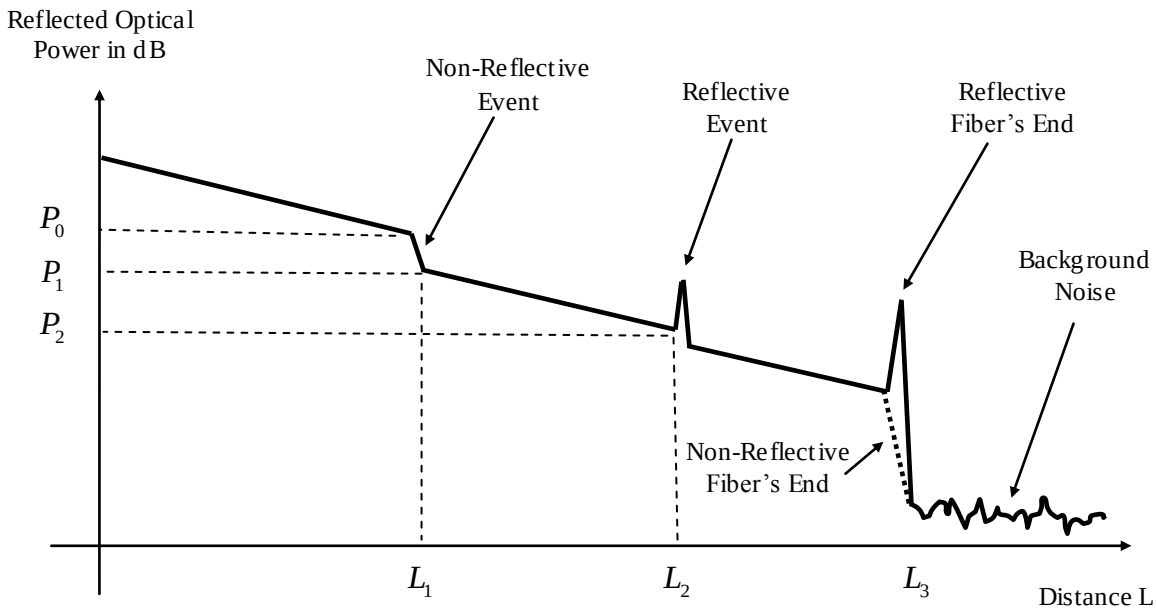

Fig. 1.1: A typical OTDR trace screen. [45]

1.2: Parameters of an OTDR:

1.2.1 Reflection:

The key to determining faults in fibres using OTDR is reflection. In an OTDR there are two types of light levels. One is a low level created by Rayleigh Backscattering and the other is a high level that is created by Fresnel Reflection. Rayleigh backscattering is used to calculate the level of attenuation in the fiber as a function of distance (expressed in dB/km), which is shown by a straight slope in an OTDR trace. This phenomenon comes from the natural reflection and absorption of impurities inside optical fiber. When hit, some particles redirect the light in different directions, creating both signal attenuation and backscattering. Higher wavelengths are less attenuated than shorter ones and, therefore, require less power to travel over the same distance in a standard fiber. The figure illustrates Rayleigh Backscattering.

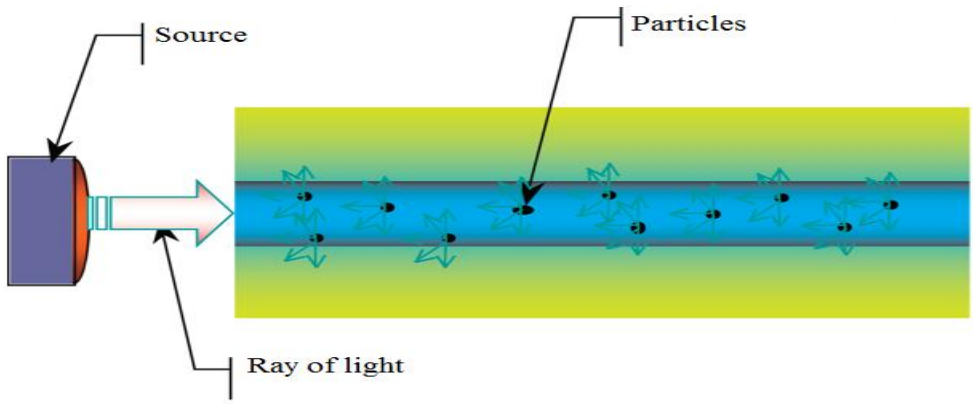

Fig.1.2: Schematic representation of Rayleigh backscattering. [45]

The second type of reflection used by an OTDR—Fresnel reflection—detects physical events along the link. When the light hits an abrupt change in index of refraction (e.g., from glass to air) a higher amount of light is reflected back, creating Fresnel reflection, which can be thousands of times bigger than the Rayleigh backscattering. Fresnel reflection is identifiable by the spikes in an OTDR trace. Examples of such reflections are connectors, mechanical splices, bulkheads, fiber breaks or opened connectors. The figure below shows how the trace detects the following events.

The 1st spike shows a mechanical splice, the 2nd spike shows a bulkhead and the 3rd

spike shows an opened connection.

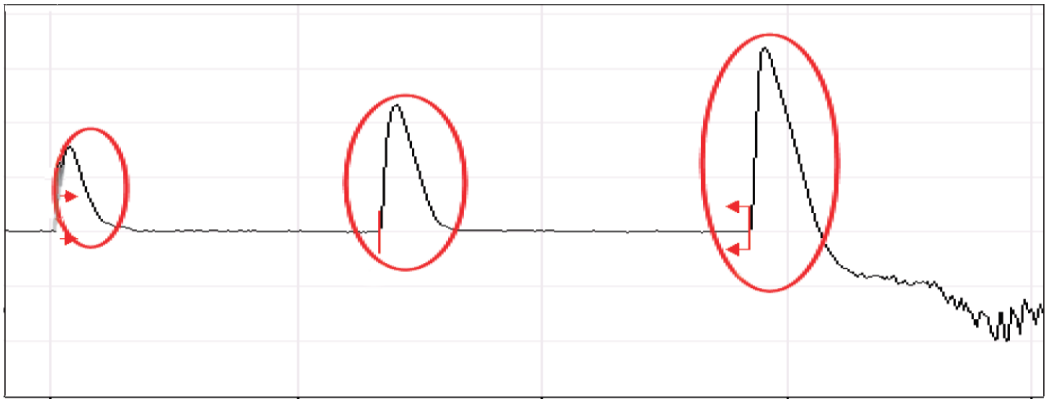

Fig. 1.3: The detected trace responses in cases of connections and open ends. [45]

1.2.2 Dead zone:

Fresnel reflections lead to an important OTDR specification known as “dead zones”. There exist two types of dead zones: event and attenuation. Both originate from Fresnel reflections and are expressed in distance (meters) that vary according to the power of those reflections. A dead zone is defined as the length of time during which the detector is temporary blinded by a high amount of reflected light, until it recovers and can read light again—think of when you drive a car at night and you cross another car in the opposite direction; your eyes are blinded for a short period of time. In the OTDR world, time is converted into distance; therefore, more reflection causes the detector to take more time to recover, resulting in a longer dead zone. Most manufacturers specify dead zones at the shortest available pulse width and on a -45 dB reflection for single mode fibers and -35 dB for multi mode fibers. There are two types of dead zones that are important in OTDRs.

1.2.2.1 Event dead zone:

The event dead zone is the minimum distance after a Fresnel reflection where an OTDR can detect another event. In other words, it is the minimum length of fiber needed between two reflective events. Still using the car example mentioned above, when your eyes are blinded by another car, after a few seconds you could notice an object on the road without being able to properly identify it. In the case of an OTDR, the consecutive event is detected, but the loss cannot be measured (as illustrated in Figure 1.4). The OTDR merges the consecutive events and returns a global reflection

and loss for all merged events. To establish specifications, the most common industry method is to measure the distance at -1.5 dB from each side of the reflective peak (see Figure 1.5). Another method that measured the distance from the beginning of the event until the reflection level falls to -1.5 dB from its peak has also been used; this method returns a longer dead zone, but it is not often used by manufacturers.

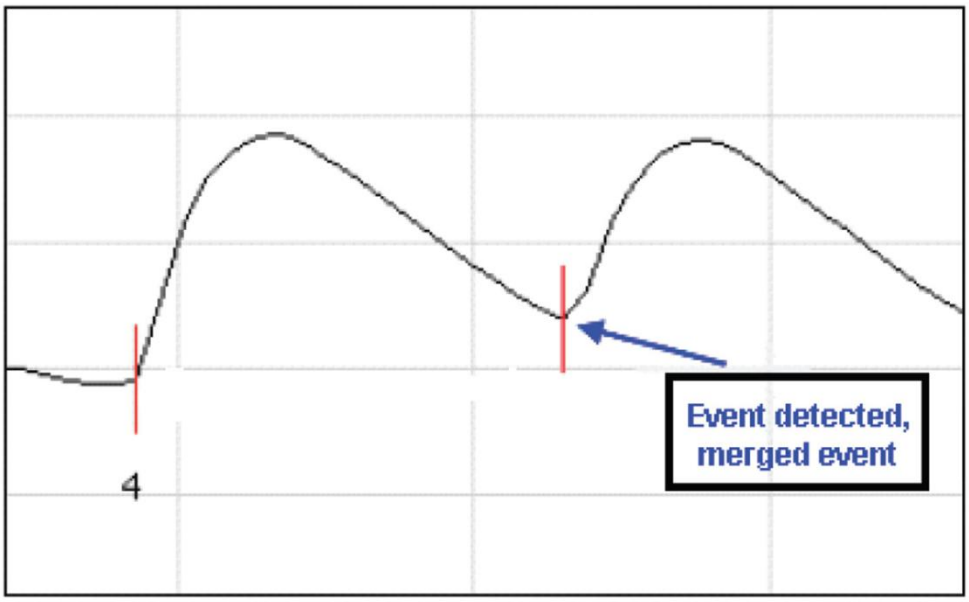

Fig. 1.4: Event dead zone in case of merged event. [45]

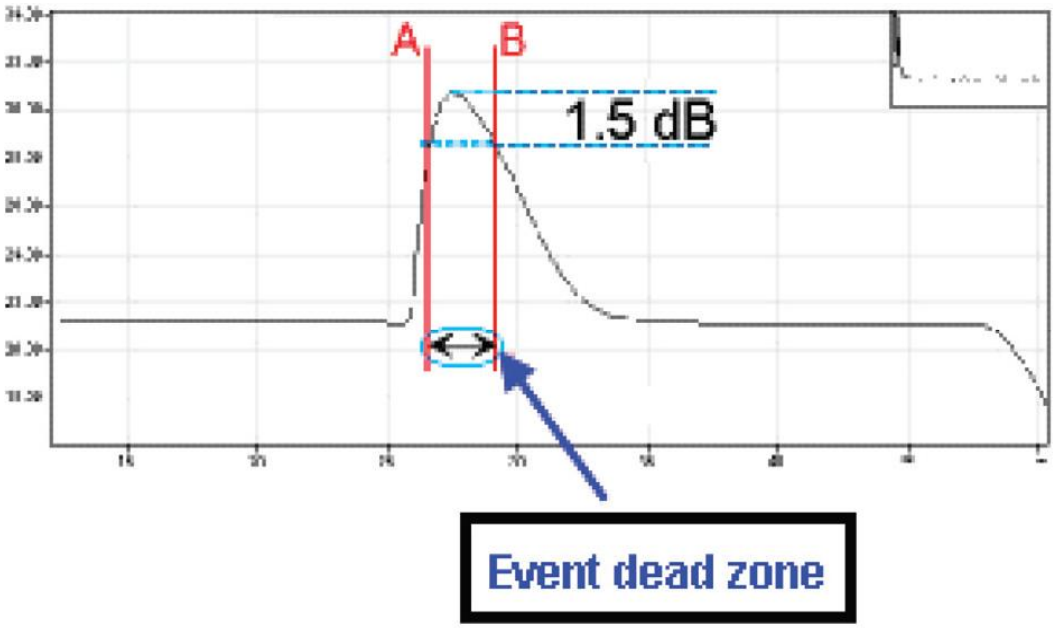

Fig. 1.5: A standard event dead zone as seen in OTDR trace. [45]

The importance of having the shortest-possible event dead zone allows the OTDR to detect closely spaced events in the link. For example, testing in premises networks

requires an OTDR with short event dead zones since the patchcords that link the various data centres are extremely short. If the dead zones are too long, some connectors may be missed and will not be identified by the technicians, which makes it harder to locate a potential problem.

1.2.2.2 Attenuation dead zones:

The attenuation dead zone is the minimum distance after a Fresnel reflection where an OTDR can accurately measure the loss of a consecutive event. Still using the car example previously mentioned, after a longer time, your eyes will have recovered enough to identify and analyze the nature of the object on the road. As illustrated in Figure 1.6 below, the detector has enough time to recover so that it can detect and measure the loss of the consecutive event. The minimum required distance is measured from the beginning of a reflective event until the reflection is back to 0.5 dB over the fiber's backscattering level, as illustrated in Figure 1.7 below.

Fig. 1.6: 1st case of attenuation dead zone. [45]

The importance of dead zones is that, short attenuation dead zones enable the OTDR to detect consecutive events that are placed close by and also to return the loss of such closely placed events. For instance, the loss of a short patchcord within a network can now be known, which helps technicians to have a clear picture of what is inside the link.

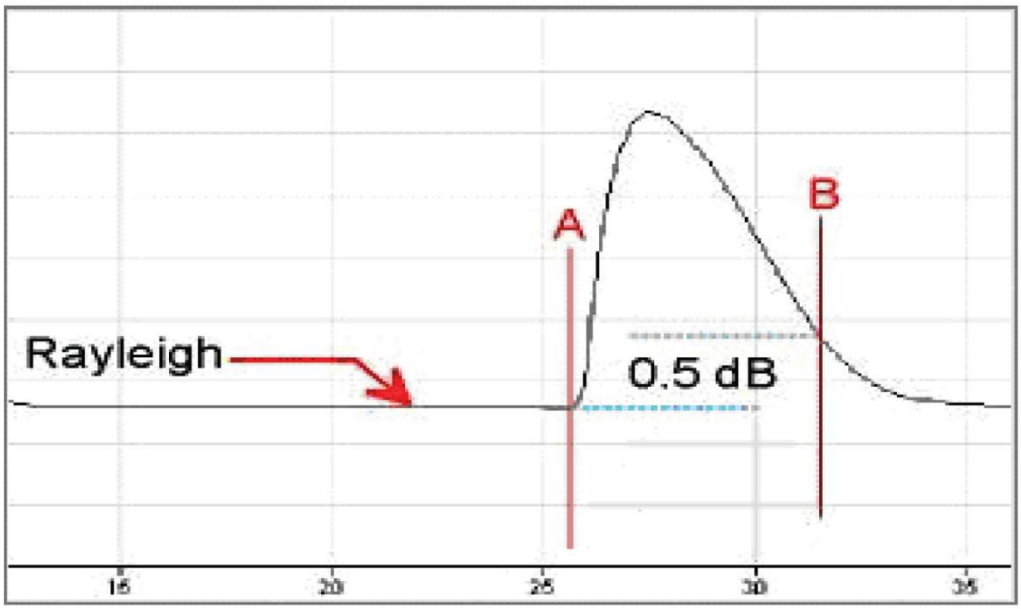

Fig. 1.7: 2nd case of attenuation dead zone. [45]

Dead zones are influenced by one more factor, namely the pulse width. Lower pulse width creates smaller dead zones and as the pulse width increases so does the dead zone. Use of longer pulse width causes larger dead zones, but the use of larger pulse width has a different advantage, which will be explained in coming sections.

1.2.3 Dynamic Range:

The third important parameter of OTDR is the dynamic range. To put it simply, dynamic range is simply the measure of the range of an OTDR, i.e. the maximum length of the fiber that the OTDR pulse can reach. This value is measured in dB and what it shows actually is the maximum loss that can be detected by the OTDR in the form of backscattering at a given noise level. Therefore, the bigger the dynamic range (in dB), the longer the distance reached. Evidently, the maximum distance varies from one application to another since the loss of the link under test is different. Connectors, splices and splitters are some of the factors that reduce the maximum length of an OTDR. Therefore, averaging for a longer period of time and using the proper distance range is the key to increasing the maximum measurable distance. Most of the dynamic range specifications are given using the longest pulse width at a three-minute averaging time, signal-to-noise ratio (SNR) = 1 (averaged level of the root mean square (RMS) noise value).

A good rule of thumb is to choose an OTDR that has a dynamic range that is 5 to 8 dB higher than the maximum loss that will be encountered. For example, a single mode OTDR with a dynamic range of 35 dB has a usable dynamic range of approximately 30 dB. Assuming typical fiber attenuation of 0.20 dB/km at 1550 nm and splices every 2 km (loss of 0.1 dB per splice), a unit such as this one will be able to accurately certify distances of up to 120 km. The maximum distance could be approximately calculated by dividing the attenuation of the fiber to the dynamic range of the OTDR. This helps determine which dynamic range will enable the unit to reach the end of the fiber. Keep in mind that the more loss there is in the network, the more dynamic range will be required. Note that a high dynamic range specified at 20 µs does not guarantee a high dynamic range at short pulses excessive trace filtration could artificially boost dynamic range at all pulses at the cost of a bad fault-finding resolution.

1.2.4 Pulse width:

What is pulse width? The pulse width is actually the time during which the laser is on. As we know, time is converted into distance so that the pulse width has a length. In an OTDR, the pulse carries the energy required to create the back reflection for link characterization. The shorter the pulse, the less energy it carries and the shorter the distance it travels due to the loss along the link (i.e., attenuation, connectors, splices, etc.). A long pulse carries much more energy for use in extremely long fibers. Figure 1.8 below illustrates the pulse width as a function of time.

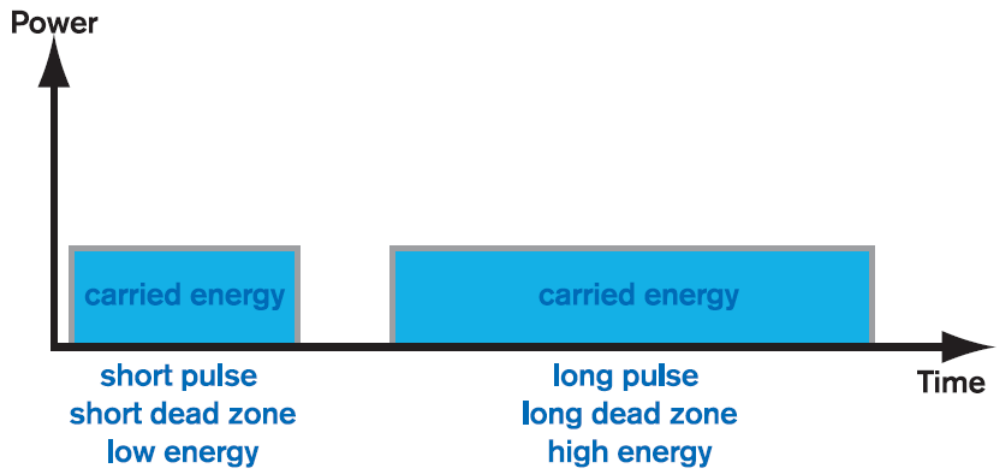

Fig. 1.8: Representation of input energy for different cases of pulses. [45]

If the pulse is too short, it loses its energy before the fiber end, causing the backscattering level to become low to the point where the information is lost at the noise floor level. This results in an inability to reach the end of the fiber. Therefore, it is not possible to measure the complete link since the returned end of fiber distance is much shorter than the actual length of the fiber. Another symptom is when the trace becomes too noisy near the fiber end; the OTDR can no longer proceed with the signal analysis and the measurements may be faulty.

So why deal with pulse width? When the trace becomes noisy, there are two easy ways to obtain a cleaner trace. First, the acquisition time can be increased, which results in a considerable improvement (increase) in SNR, while maintaining the good resolution of the short pulse. However, increasing the averaging time has its limits, as it does not improve SNR indefinitely. If the trace is still not sufficiently smooth, then we move on to the second method, which is to use the next available higher pulse (more energy). However, keep in mind that dead zones extend along with the pulse width. Fortunately, most OTDRs on the market have an Auto mode that selects the appropriate pulse width for the fiber under test; this option is very convenient when the length or loss of the fiber under test is unknown.

When characterizing a network or a fiber, it is mandatory to select the right pulse width for the link under test. Short pulse width, short dead zone and low power are used to test short links where events are closely spaced, while a long pulse width, long dead zone and high power are used to reach further distances for longer networks or high-loss networks.

1.2.5 Sampling resolution and sampling points:

The ability for an OTDR to pinpoint the right distance of an event relies on a combination of different parameters and among them are the sampling resolution and the sampling points. Sampling resolution is defined as “the minimum distance between two consecutive sampling points acquired by the instrument”. This parameter is crucial, as it defines the ultimate distance accuracy and fault-finding capability of the OTDR. Depending on the selected pulse width and distance range, this value could vary from 4 cm up to a few meters. Consequently, there must be a high number of sampling points taken during an acquisition to maintain the best possible resolution. Figures 1.9 and 1.10 illustrate the role that high resolution plays in fault-

finding.

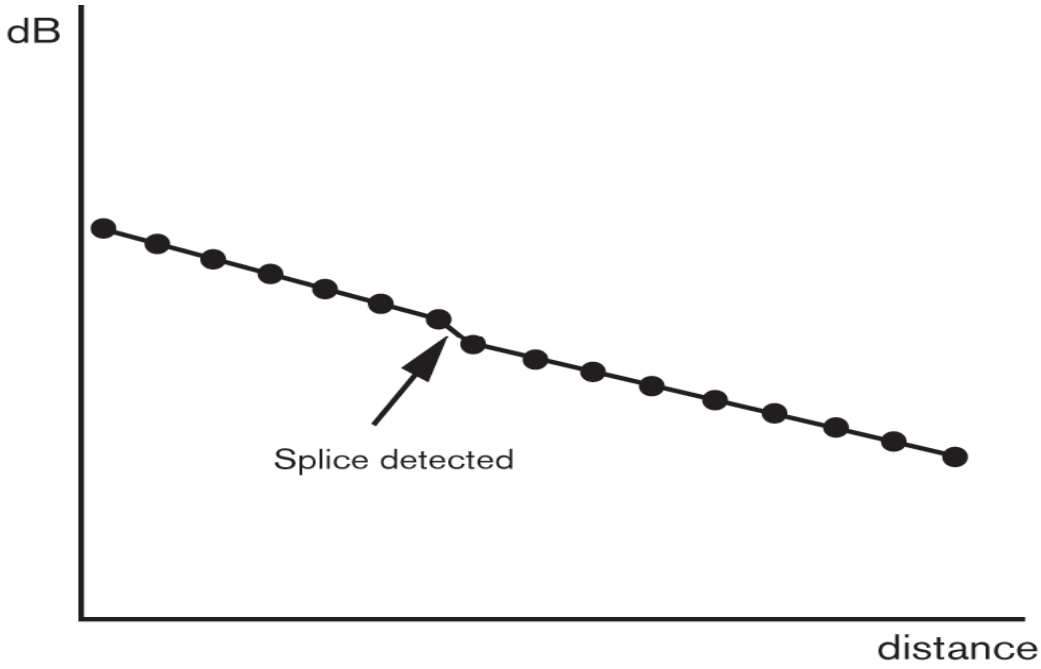

Fig. 1.9: Fault detection in high resolution cases. [45]

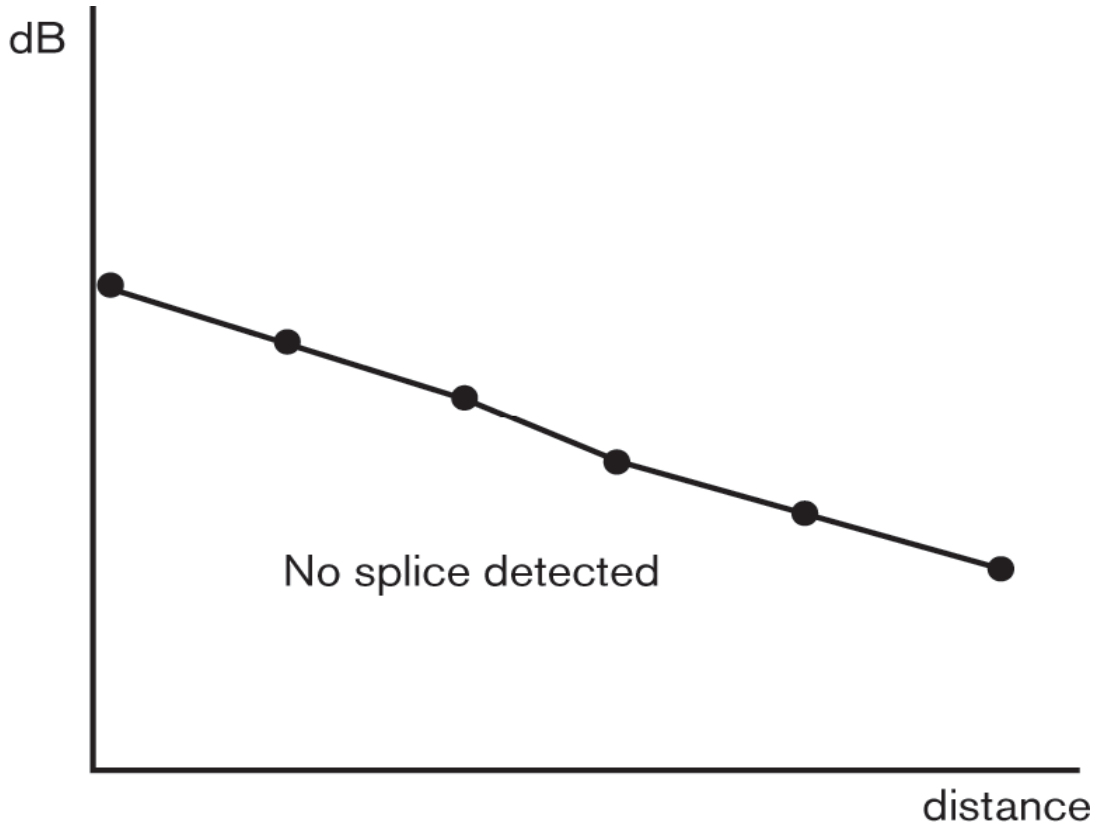

Fig. 1.10: Fault detection in low resolution cases. [45]

These are the various parameters of an OTDR that influence its operation and efficiency. While designing an OTDR, manufacturers pay maximum attention to these

details so that their design can perform even under difficult circumstances. Next we will see the different coding techniques used in OTDR systems.

1.3 Conclusion:

In this chapter we have seen the different aspects of OTDR and what are the different criteria to be considered while designing or selection of one for research or for practical purposes.

CHAPTER 2

INTRODUCTION AND MATHEMATICAL ANALYSIS OF DIFFERENT CODING TECHNIQUES

2.1 Introduction to coding:

Coding tackles the two major parameters of an OTDR, namely dead zone and pulse width. As we have seen in the pulse width section, we need more energy in the signal that the OTDR sends in order to detect faults in extremely long fibers. By incorporating a code of a length of, say 64 bits, we are in fact sending that many pulses into the fiber and hence input that much energy into the fiber and hence we can improve the SNR of the OTDR as increasing signal power for the same level of noise results in larger SNR. Also the dead zone problem is also accounted for as in coding the no of pulses are increased and not the pulse width in itself.

OTDR is an important diagnostic tool for the testing of fiber optic transmission system. At present time when optical fiber technology is widely applied not only in building up of optical fiber transmission systems but also in other fields like sensors with distributed parameters "Optical Time-Domain Reflectometry" (OTDR) plays an important role. The basic idea of the conventional OTDR consists in launching a rather short and high power optical impulse into the tested fiber and the consequent detection of the Rayleigh back-scattered or Fresnel reflected light at the input end of the fiber. The measured signal is very weak – typically 40-60 dB under the level of the launched optical power. In OTDR there is also a well-known trade-off between the Signal-Noise Ratio (SNR) and the spatial resolution. Increasing the pulse width of the probe pulse improves the signal-to-noise ratio (SNR) of the detected signal and accordingly improves the dynamic range but degrades the spatial resolution of the OTDR. To overcome this tradeoff between the SNR and the spatial resolution, the use of correlation techniques—commonly used in wireless radars—have been suggested, e.g., employing periodic pseudorandom bit sequences (PRBSs). Still, with the problem resulting from the periodic features of PRBS, this approach was found to be unsuitable for the practical applications. Overcoming the limitations of PRBS-coded OTDR, the complementary correlation OTDR (cc-OTDR) based on the Golay codes was suggested. Following the cc-OTDR, an OTDR based on the simplex codes (scs), Biorthogonal codes, correlated Prometheus orthonormal sequence was then proposed, predicting better SNR performances (over the Golay-code cc-OTDR) without the penalty in the spatial resolution. Still, with the analysis based on simple analogy—compared to that of optical spectrometry the scope of the work was limited to a conjecture on the expected amount of coding gain (SNR increase over conventional

OTDR, with identical measurement time and spatial resolution). Therefore researchers are permanently trying to look for new ways how to remove this limitation and also new approaches how to enhance its performance parameters. The performance parameters of this method are limited mainly by the SNR. One of the most effective ways for its improvement is the use of the coded test signals. Another parameter related to SNR is the peak to average power ratio (PAPR). In this paper we give a brief overview of the latest developments in the application of the coded-probe signal approaches to the SNR enhancement in OTDR.

2.2. SNR in the conventional OTDR :

Let P_{bst} (t) be the reflectivity of a fiber of particular length. Reflectivity is calculated by injecting the optical power, in the form of electrical voltage or current, into the fiber at one end and measuring the reflected signal at same end as a function of time or distance. This method of injection is carried out several times and the result is averaged. Let P_{bsm} (t) be the back-scattered optical power detected at the input end of the fiber as a response to a short and high power level probe optical impulse injected into the probed fiber. This reflected signal is somewhat different from the injected pulse due to the presence of noise, so that P_{bsm} (t) = P_{bst} (t) + e, where e is the noise amplitude [4]. The variance of the measurement is given by quadratic mean-square value as follows $[P_{bsm}(t) - P_{bst}(t)]^2 = e^2 = \sigma^2$ that represents the electrical noise power in the measurements. If the measurement is repeated N times and let the noise is uncorrelated zero mean random variable then the mean value of P_{bsm} (t) is given as

$$P_{bsm}(t) = \frac{1}{N}\sum_{i=0}^{N} P_{bsm(i)}(t) = P_{bst} + \frac{1}{N}\sum_{i=1}^{N} e_i \qquad (2.1)$$

Now the variance in the measurement is

$$[P_{bsm}(t) - P_{bst}(t)]^2 = \frac{1}{N^2}\left(\sum_{i=1}^{N} e_i\right)^2 = \frac{\sigma^2}{N} \qquad (2.2)$$

Thus the noise power of the N times repeated measurement process is reduced by the factor N or consequently the noise amplitude is also decreased by the factor $\sqrt{N}$. Due to the fact that the total detected signal amplitude is proportional to the N the SNR of the conventional OTDR is enhanced by the factor of $\sqrt{N}$.

Peak to Average Power Ratio (also known as Peak to Mean Envelope Power Ratio or PMEPR) is a metric of wireless signals which define the variations in the transmit power for that signal. Large variations in output power i.e. large PAPR are a cause of concern; they can cause power amplifier (PA) saturation, non-linearity and other effects. To combat this, the power amplifier has to operate in the linear range; this in turn causes significant inefficiency of operation and requires more expensive PAs. In OTDR, codes with low PAPR helps in launching more power into the fiber and hence increase the SNR.

For any codeword c, the instantaneous power of the corresponding transmitted signal $S_c(t)$ is equal to $|S_c(t)|^2$.The average power is given by $\|c\|^2$ where $\|.\|$ is the Euclidean norm. So PAPR of the codeword can be given as

$$\text{PAPR} \leq \max \frac{|Sc(t)|^2}{\|c\|^2} \qquad (2.3)$$

Similarly for any code 'c' of length n, rate R and Euclidean distance d, the PAPR is given as

$$\text{PAPR} \geq n\,(1-d_*^2/2n)^2 \qquad (2.4)$$

Where d_* denotes the minimum distance between the code words of c.

2.3 Different Codes used in OTDR:

In OTDR the following codes have been successfully implemented so far.

2.3.1. Golay Codes (GC):

2.3.1.1 Introduction to Golay codes:

The Golay code is one of the most important types of linear binary block codes. It is of particular significance since it is one of only a few examples of a nontrivial perfect code. The Golay code is actually an error correcting code that is widely used in digital communication and was the first code to have been incorporated with an OTDR. Its fundamental with respect to error correction is that a t-error-correcting code can correct a maximum of t errors. A perfect t-error correcting code has the property that every word lies within a distance of t to exactly one code word. Therefore, the code has $d_{min} = 2t + 1$, and a covering radius t, where the covering radius r is the smallest

number such that every word lies within a distance of r to a codeword. This table shows us a few Golay codes.

Code Length	X(X*)	Y(Y*)	Amplitude of the main peak
2	+ +(+ +)	+ -(- +)	4
4	+ + - +(+ - + +)	+ + + -(- + + +)	8
8	+ + + - + + - + (+ - + + - + + +)	+ + + - - - + - (- + - - - + + +)	16
16	- - + - - - - + - + + + + - + - - (- - + - + + + + - + - - - - + - -)	- - + - - - - + + - - - + - + + (+ + - + - - - + + - - - - + - -)	32

Table 2.1. A few examples of Golay Codes.

Where X* and Y* are code sequences applied for the compression using matched filters

2.3.1.2 Construction of Golay Code (GC)

It is truly the bipolar code with the amplitudes of +1 and -1, consisting of two complementary components *A* and *B*, each of them being of the same bit length *L*. The most valuable property of the code is represented by the fact that the sum of the autocorrelation functions of the both components is proportional to the δ (*t*) function. This code can be described by the relation

$$A \otimes A + B \otimes B = 2L\delta(t) \qquad (2.5)$$

The recursive rule for the generation of the complementary pair of the code was introduced by M. J. E. Golay. According to the rule it is possible to generate from the components *A*, *B* of an *L*-bit pair of the bipolar Golay code a new 2*L*-bit pair code in the following manner

$$\begin{pmatrix} A \\ B \end{pmatrix} \rightarrow \begin{pmatrix} A & B \\ A & \overline{B} \end{pmatrix}$$

where $\overline{B}$ represents complementary value to the *B*. This procedure allows create codes with the required bit length. The number of bits of the code is given by the power of 2. Below is shown the construction of the two-, four- and eight-bit code from the one-bit code for $A = [1]$, $B = [1]$

$$\begin{pmatrix} 1 \\ 1 \end{pmatrix} \rightarrow \begin{pmatrix} 1 & 1 \\ 1 & -1 \end{pmatrix} \rightarrow \begin{pmatrix} 1 & 1 & 1 & -1 \\ 1 & 1 & -1 & 1 \end{pmatrix} \rightarrow$$

$$\rightarrow \begin{pmatrix} 1 & 1 & 1 & -1 & 1 & 1 & -1 & 1 \\ 1 & 1 & 1 & -1 & -1 & -1 & 1 & -1 \end{pmatrix}$$

2.3.1.3 OTDR based on the use of the Golay Code (GC OTDR)

The principle of the OTDR based on the application of the Golay code (GC) consists in probing the fiber by a continuous optical signal modulated by the GC function. Due to the fact that the probing signal is spread in longer time it is possible to launch much more energy into the fiber as compared with the case of a single impulse as it is in conventional OTDR. Nearly the same space resolution as it is in conventional OTDR is obtained by the use of the autocorrelation function of the GC. By performing the correlation between the modulation signal and the back-scattered signal it is possible to restore the backscattered power. It is equivalent to the response corresponding to probing the fiber by one impulse of the GC but with the optical power multiplied by the number L which is the length of the GC (number of impulses in one sequence of the GC). GC is a bipolar code in which only two values +1 and –1 occur, but we know that for OTDR the coded signal used should be unipolar in nature. Due to the fact that the optical power can not be of "negative" value it is necessary to probe the fiber by four modified components of the GC as follows A1, A2, B1, B2 that are defined by the relations A1=0.5(1+A), A2 =0.5(1-A), B1=0.5(1+B), B2=0.5(1-B) [1]. Simultaneously it holds A=A1-A2, B=B1-B2. One can easily show that these signals do not contain any negative values and as a result they can be realized by the

modulation of optical power. After the detection of the fiber responses to these N-times repeated application of the four probe signals and a consequent arithmetic averaging one has to calculate the correlation function between the averaged signals and the particular GC components A and B respectively. The resulting signal - the time dependence of the back-scattered signal - is given by the sum of these correlation functions [6].

The SNR of the GC-OTDR with the code length of L bits is defined by the relation that is frequently named as OTDR maker´s formula

$$\text{SNR (dB)} = P_{in} - P_{NEP} + 1.5 \times (N_{oct} + L_{oct}) - 2 \times a \times z \qquad (2.6)$$

where P_{in} is the optical power of the input test impulse, P_{NEP} is noise equivalent power of the optical receiver $N_{oct} = \log_2 N$ while N is the number of measurements during the averaging process and $L_{oct} = \log_2 L$, where L is the GC length, 'a' the attenuation coefficient of the fiber and 'z' is the distance from the input end of the fiber.

By comparing the performance parameters of the conventional OTDR and the GC-OTDR one can state that the SNR and consequently also the dynamical range of the GC-OTDR is $\sqrt{\frac{L}{4}}$ times better than it is in conventional OTDR provided the available impulse optical power of the laser is the same in both cases. Also the PAPR of any Golay code is at most 2 which is quite low.

2.3.2 Biorthogonal Codes:

2.3.3.1 Introduction to Biorthogonal Codes:

Many experimental demonstrations of SNR improvement using the coding techniques have been limited to the complementary correlation OTDR based on the Golay codes [27]. These however suffer from a spatial resolution penalty that results in a reduction of SNR by around 3-dB at the same level of spatial resolution. These processes are inherently associated with the decoding process of the correlation OTDR [29].It was however shown that it is possible to avoid this penalty of 3-dB by preserving the shape of the unit pulse in the decoding process with a proper code set and decoding method based on the linear matrix operations of addition and subtraction. The resulting coding sequence is what is called a Bi-orthogonal sequence and this method

of coding has been proven to have significant impact on the SNR improvement of OTDR systems.

Biorthogonal code is a kind of error correcting codes and consists of a combination of orthogonal and antipodal signals. When the code length is n, a Biorthogonal code set has 2n code words constituting a 2n × n BC matrix B. In contrast with the correlation approach discussed above OTDR based on the use of orthogonal codes (OC) utilizes the basic properties of the direct and inverse linear transformation of the OC. At this approach the optical fiber is repeatedly probed by a set of series optical impulses (code words) with the sequence in one code word defined by a particular BC. The basic idea of the method consists in detection of the back-scattered power coming simultaneously from different points on the fiber. It is achieved by the time delay between the particular bits of the code word of the BC.

2.3.2.2 Construction of Bi-orthogonal Code:

In the following we shall briefly describe the BC construction using the Hadamard matrix (HM) [1]. The basic HM – H_1 has the form

$$H_1 = \begin{pmatrix} 0 & 0 \\ 0 & 1 \end{pmatrix}$$

The higher order HM can be generated by the application of the C formula

$$H_m = \begin{pmatrix} H_{m-1} & H_{m-1} \\ H_{m-1} & H'_{m-1} \end{pmatrix}$$

where the symbol ' means that the matrix is a complementary to the matrix H. Using the HM H_m one can construct the Biorthogonal code matrix B_m consisting of 2n lines (code words) of the length n as follows

$$B=B_m = \begin{pmatrix} H_m \\ H'_m \end{pmatrix}$$

The code word length n is related to the matrix index m through the relation $n = 2m$. It is interesting that the matrix H_m has several significant properties - except the first line and column its lines represent the orthogonal vectors, the number of units and zeros in the word is the same, the matrix is symmetrical.

2.3.2.3 OTDR based on the use of Biorthogonal Code

We measure the fiber under test by launching n-bit coded pulse sequences 2n times sequentially, according to the constructed Biorthogonal code words. Then the original OTDR trace is restored from the 2n measured traces, using the Moore-Penrose generalized inverses. Since the rows of B are linearly independent, the generalized inverses [2] B^{+} can be calculated by $B^{+}= (B^{T}B)^{-1}B^{T}$, where B^{T} and B^{-1} means the transpose and the inverse of the matrix B, respectively. The restored trace shows the same shape as the conventional OTDR trace which is averaged from 2n single pulse measurements, except for its improved SNR achieved from the higher backscatter level in each measurement by launching n-bit pulse sequences rather than a single pulse into the fiber. The equation below shows an example using 2-bit Biorthogonal code set which has 4 code words:

$$\begin{pmatrix} \eta_1(t) \\ \eta_2(t) \\ \eta_3(t) \\ \eta_4(t) \end{pmatrix} = B \begin{pmatrix} \psi_1(t) \\ \psi_2(t) \end{pmatrix} + \begin{pmatrix} e_1(t) \\ e_2(t) \\ e_3(t) \\ e_4(t) \end{pmatrix}, \quad B = \begin{pmatrix} 0 & 0 \\ 0 & 1 \\ 1 & 1 \\ 1 & 0 \end{pmatrix} \tag{2.7}$$

When ψ_1 represents a conventional OTDR trace obtained by launching a single pulse into fiber, let us define $\psi_n(t)$ as the time delayed version of $\psi_1(t)$, $\psi_n(t) = \psi_1(t-(n-1)\tau)$, where τ is the pulse width of the single pulse. Then $\eta_1(t)$ and $e_i(t)$ represents the trace measured with i^{th} codeword and noise amplitude added in each measurement, respectively.

Figure below shows examples of probe pulses with 2 bit bi-orthogonal code sets.

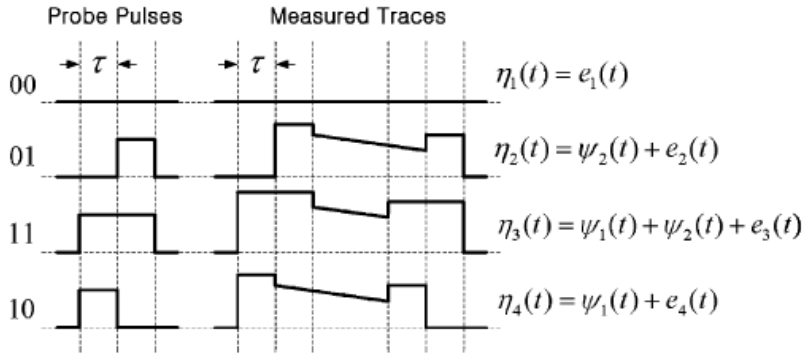

Fig. 2.1: Pulse generation used in bi-orthogonal codes [2]

In order to recover the original OTDR trace $\psi_1(t)$ from these measured traces, Moore-Penrose generalized inverse of the Biorthogonal code matrix B is multiplied to the matrix of the measured traces as shown below, where $\hat{\psi}_i(t)$ represents the estimate of $\psi_i(t)$:

$$\begin{pmatrix}\hat{\psi}_1(t)\\ \hat{\psi}_2(t)\end{pmatrix} = B^{+}\begin{pmatrix}\eta_1(t)\\ \eta_2(t)\\ \eta_3(t)\\ \eta_4(t)\end{pmatrix} = \begin{pmatrix}\psi_1(t)\\ \psi_2(t)\end{pmatrix} + B^{+}\begin{pmatrix}e_1(t)\\ e_2(t)\\ e_3(t)\\ e_4(t)\end{pmatrix} \tag{2.8}$$

$$\begin{pmatrix}\hat{\psi}_1(t)\\ \hat{\psi}_2(t)\end{pmatrix} = B^{+}\begin{pmatrix}0\\ \eta_2(t)\\ \eta_2(t)+\eta_4(t)\\ \eta_4(t)\end{pmatrix} = \begin{pmatrix}\psi_1(t)\\ \psi_2(t)\end{pmatrix} + B^{+}_{eff}\begin{pmatrix}e_1(t)\\ e_2(t)\\ e_3(t)\\ e_4(t)\end{pmatrix} \tag{2.9}$$

where $B^{+} = \frac{1}{3}\begin{pmatrix}0 & -1 & 1 & 2\\ 0 & 2 & 1 & -1\end{pmatrix}$, $B^{+}_{eff} = \frac{1}{3}\begin{pmatrix}0 & 0 & 0 & 3\\ 0 & 3 & 0 & 0\end{pmatrix}$

By expanding first equation it is found that η_1 and η_2 are unnecessary because η_1 only has noise signals and $\eta_3(t)$ can be substituted with a summation of other measurements $\eta_2(t)$ and $\eta_4(t)$. Even in the case of code length n, we can omit two measurements η_1 and η_{n+1}, by using $\eta_1=0$ and $\eta_{n+1}(t) + \eta_{n/2+1} + \eta_{3n/2+1}(t)$. Note that the matrix B^{+}_{eff}, which is effectively applied to the noise matrix, is different from the original generalized inverse. B^{+} is obtained after replacing $\eta_3(t) = \eta_2(t) + \eta_4(t)$.

As we defined $\psi_n(t)$ as the time delayed version of $\psi_1(t)$, the finally restored trace with maximum SNR can be obtained by

$$\frac{\hat{\Psi}_1(t) + \hat{\Psi}_2(t+\tau)}{2} = \psi_1(t) + \frac{e_4(t) + e_2(t) + e_3(t)}{2} \tag{2.10}$$

The coding gain for the general code length 'n' can be calculated using the matrix B_{eff}^{+} which is effectively applied to the noise matrix as in above equation. Finally the coding gain can be obtained calculating the ratio of noise amplitude between the coding OTDR and conventional OTDR. Now for an 'n' bit code the noise power in each estimate $\hat{\Psi}_j(t)$ is given as

$$\sum_{j=1}^{2n}\left(b_{i,j}^{+}\right)^2 = \frac{2n^3+2n^2+12}{n^2(n+1)^2}\ , i = 1,2,\ldots\ldots,n \tag{2.11}$$

Where $b_{i,j}^{+}$ represents an (i,j) element of the matrix B_{eff}^{+}.

Then the coding gain [2] at the code length 'n' becomes

$$\sqrt{\frac{\frac{\sigma^2}{2n-2}}{\frac{2n^3+2n^2+12}{n^3(n+1)^2}}} = \sqrt{\frac{n^3(n+1)^2}{4(n+1)(n^3+n^2+6)}} \tag{2.12}$$

Here it is assumed that noise is uncorrelated, zero mean random variable with variance (σ^2). Application of biorthogonal code in OTDR made it possible to improve the SNR by an amount of 10dB against the conventional OTDR for length L=256.

Figure below here shows difference in code gain of bi-orthogonal codes from normal Golay codes.

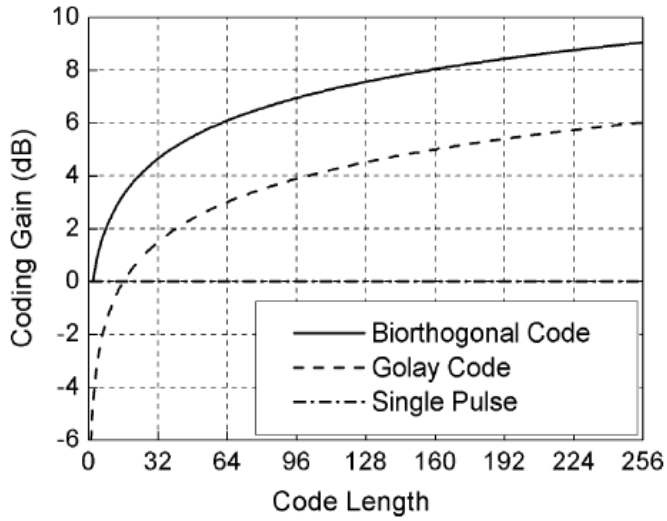

Fig. 2.2: Code gain comparison of bi-orthogonal code with Golay code. [2]

2.3.3 Simplex Codes:

2.3.3.1 Introduction to Simplex Codes:

We know that an optical time-domain reflectometer (OTDR) characterizes optical fibres by injecting an optical probe pulse into the fiber under test and detecting the backscattered optical signals. By increasing the pulse width of the input pulse we can improve the signal-to-noise ratio (SNR) of the detected signal and accordingly improve the dynamic range. But this degrades the spatial resolution of the OTDR. To overcome this trade-off between the SNR and the spatial resolution, the most common method used is correlation techniques. The use of these techniques in wireless radars has been the most and the method involves the employment of periodic pseudorandom bit sequences (PRBS) [24], [25]. Still, problems began to rise from the periodic features of PRBS and this approach was found to be unsuitable for the practical applications [26]. Hence, to overcome the limitations of PRBS-coded OTDR, the method of complementary correlation OTDR (cc-OTDR), which is based on the Golay codes, was suggested [27]. Following the introduction of cc-OTDR, an OTDR based on the simplex codes (scs) was then proposed [28]. The implementation of Simplex Code based OTDR predicted better SNR performances over the Golay-code cc-OTDR without the resulting penalty in the spatial resolution. Still, this analysis was based on simple analogy, compared to that of optical spectrometry [29],[30]. The scope of this work was limited to a conjecture on the expected amount of coding gain, i.e. the SNR increase of the Simplex Code based OTDR over a

conventional OTDR, with identical measurement times and spatial resolutions. In consideration with the need of a detailed set of guidelines for its practical application, a systematic analysis of the system, with considerations on OTDR-specific hardware, and the resulting experimental data was to be provided to give insights for the initial design consideration.

2.3.3.2 Construction of Simplex Code

Simplex code is also constructed from Hadamard code. Hadamard code is the basis of construction of all codes. The S-codes are the rows of an M×M matrix S called the S-matrix which is obtained from the Hadamard matrix of order M+1 by omitting the first row and first column.

2.3.3.3 SNR improvement of OTDR using Simplex Code

Let us consider a simplex code of length L [3].Let $\psi_1(t)$ be the OTDR trace measured with single probe pulse and $\psi_2(t)$,$\psi_L(t)$ are the delayed version of the pulses such that

$$\psi_2(t) = \psi_1(t-\tau)\ ,\psi_3(t) = \psi_1(t-2\tau), \psi_L(t) = \psi_1(t-(L-1)\tau) \qquad (2.13)$$

Let $\hat{\Psi}_L(t)$ be the estimated trace of the OTDR. Then writing S_L and S_L^{-1} as S matrix and its inverse matrix of order L, trace estimates can be written as

$$\begin{pmatrix} \hat{\Psi}_1(t) \\ \hat{\psi}_2(t) \\ \vdots \\ \hat{\Psi}_L(t) \end{pmatrix} = S_L^{-1}\begin{pmatrix} \eta_1(t) \\ \eta_2(t) \\ \vdots \\ \eta_L(t) \end{pmatrix} = \begin{pmatrix} \psi_1(t) \\ \psi_2(t) \\ \vdots \\ \psi_L(t) \end{pmatrix} + S_L^{-1}\begin{pmatrix} e_1(t) \\ e_2(t) \\ \vdots \\ e_L(t) \end{pmatrix} \qquad (2.14)$$

Now, inversely time shifting each row in above expression with multiples of t, and then introducing matrix T_L (normalized matrix of S_L^{-1}), we obtain the following equation

$$\begin{pmatrix} \hat{\Psi}_1(t) \\ \hat{\psi}_2(t+\tau) \\ \vdots \\ \hat{\Psi}_L(t+(L-1)\tau) \end{pmatrix} = \begin{pmatrix} \psi_1(t) \\ \psi_2(t+\tau) \\ \vdots \\ \psi_L(t+(L-1)\tau) \end{pmatrix} + \frac{2}{L+1} T_L \begin{pmatrix} e_1(t) \\ e_2(t+\tau) \\ \vdots \\ e_L(t+(L-1)\tau) \end{pmatrix}$$

Where $$T_L = L + \frac{1}{2} * S_L^{-1}, T_{j,k} \in \{1, -1\} \qquad (2.15)$$

Now, utilizing the following relation

$\Psi_i (t+ (i+1) \tau) = \Psi_1(t)$ $(i = 1,2,3 \ldots\ldots\ldots\ldots L)$ (2.16)

we obtain L equations relating the estimate $\psi_i(t)$ to the conventional trace $\psi_1(t)$ as

$$\widehat{\Psi_1}(t) = \Psi_1(t) + \frac{2}{L+1}\sum_{k=1}^{L} T_{1,k} e_k(t) \quad (2.17)$$

$$\widehat{\Psi_2}(t+\tau) = \Psi_1(t) + \frac{2}{L+1}\sum_{k=1}^{L} T_{1,k} e_k(t+\tau) \quad (2.18)$$

$$\vdots$$

$$\widehat{\Psi_L}(t + (L-1)\tau) = \Psi_1(t) + \frac{2}{L+1}\sum_{k=1}^{L} T_{L,k} e_k *(t+(L-1)\tau) \quad (2.19)$$

Finally, summing over the traces and taking its average, the following equation for the final trace can be obtained, which includes the exact noise components:

$$\frac{1}{L}\sum_{k=1}^{L} \widehat{\Psi_k}(t+(k-1)\tau) = \Psi_1(t) + \frac{2}{L(L+1)}\sum_{j=1}^{L} T_{j,k} e_k(t+(L-1)\tau) \quad (2.20)$$

Now, calculating the mse of the restored trace

$$E\left\{\left(\frac{1}{L}\sum_{k=1}^{L} \widehat{\Psi_k}(t+(k-1)\tau) - \Psi_1(t)\right)^2\right\} = \frac{4}{L^2(L+1)^2} E\left\{\left(\sum_{j=1}^{L}\sum_{k=1}^{L} T_{j,k} e_k(t+(L-1)\tau)\right)^2\right\} \quad (2.21)$$

$$= \frac{4}{L^2(L+1)^2} E\left\{L^2\sigma^2 - \sum_{i=1}^{L-1}(L-1)R_N(i\tau)\right\}$$

$$= \frac{4}{L^2(L+1)^2}\left\{\sigma^2 - \frac{1}{L^2}\sum_{i=1}^{L-1}(L-i)R_N(i\tau)\right\}$$

Note that the above result was derived by using the following assumptions:

$E\{e_i(t+\zeta)\} = 0$

$E\{e_i^2(t+\zeta)\} = \sigma^2$

$E\{e_i(t)\, e_j(t+\zeta)\} = 0 \ (i \neq j)$

$E\{e_i(t)\, e_j(t+\zeta)\} = R_i(\zeta)$

$= R_N(\zeta) \qquad (i=1, 2\ldots\ldots L)$

I.e. noise is uncorrelated

Restricting our analysis to an ideal receiver with an infinite bandwidth, the mse can be simplified to

$$\frac{4\sigma^2}{(\mathbf{L}+1)^2} \tag{2.22}$$

Finally the expression for the coding gain [3] of an SC OTDR of length=L can be written as

$$\frac{\sqrt{\frac{\sigma^2}{L}}}{\sqrt{\left(\frac{4\sigma^2}{L+1}\right)^2}} = \frac{L+1}{2\sqrt{L}} \tag{2.23}$$

Application of simplex code to OTDR also resulted a increase in coding gain. Experiments have been carried out for a simplex code of length 7 the code gain was found to be 2.3 dB and for a length of L=255 the code gain was found to be 9.2dB. Figure below shows how the code gain of Simplex codes vary with code length

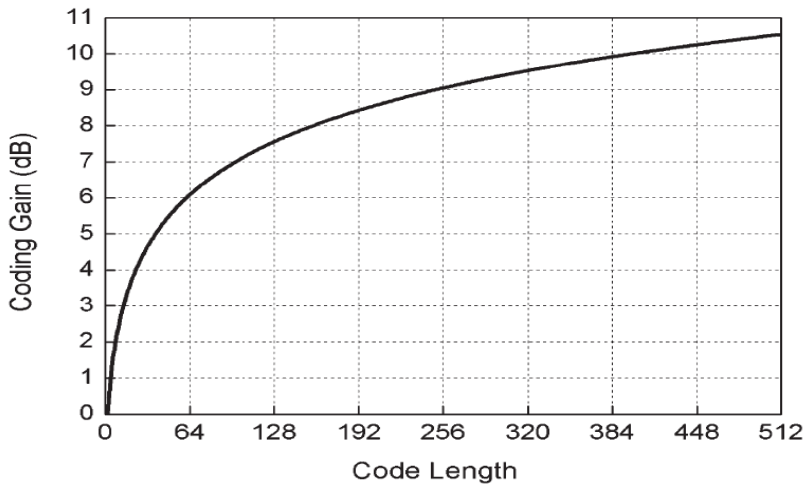

Fig. 2.3 Coding gain in Case of Simplex Codes.[4]

2.3.4. CCPONS:

2.3.4.1 Introduction to CCPONS

CCPONS stands for Complementary Correlated Prometheus Non-Orthogonal Sequence. It is one of the latest coding sequences to be integrated with an OTDR. An OTDR system, exploiting for the use of the CCPONS, provides strongly enhanced

performance in terms of the dynamic range and SNR. The coding and decoding operations in CCPONS utilize exclusively a set of integer additions and subtractions. Here, we have used a complementary quartet of the codes. Coding in OTDR has to be unipolar as polar signal sources can induce polarity based scattering in fibres. Also, the OTDR needs to have coding schemes that can be detected by a direct detection module. For this purpose, we have obtained the unipolar version of the required quartet and we transmit a unipolar version of the codes and their 1's complement version. The main advantage of this coding is the low Crest Factor. Crest factor is a description of the extent of extreme fluctuations in signal power over time. This enables us to launch more energy into the fibre and hence improve the SNR.

Following the CCPONS equations, the variation of code gain with respect to code length can be obtained quite easily. We can see that the CCPONS coded sequence produces an impressive result compared to the single pulse case. In addition, the CCPONS coding has an advantage that it requires only the transmission of four complementary codes or quartet of codes and their 1's complement versions. Therefore this process reduces the systems processing time when compared with other codes like Hadamard codes, Simplex codes, Bi-orthogonal codes and Golay codes. In those cases it is required to transmit a matrix of codes and the code length is dependent on the size of the matrix, I.e. the number of rows in the matrix . Also, it is possible to generate different quartets of CCPONS and hence supports a multitasking

2.3.4.2 Construction of PONS

The PONS construction technique is based upon ideas of Golay and Shapiro. Golay and Shapiro method starts with the a matrix of two rows representing a pair of complementary codes,

$$\begin{pmatrix} p_1^{(1)} \\ p_2^{(1)} \end{pmatrix} = \begin{pmatrix} 1 & 1 \\ 1 & -1 \end{pmatrix}$$

Longer complementary codes of length any power of 2 are generated by the following scheme:

$$\begin{pmatrix} p_1^{(1)} \\ p_2^{(1)} \end{pmatrix} = \begin{pmatrix} p_1^{(k-1)} & p_2^{(k-1)} \\ p_1^{(k-1)} & -p_2^{(k-1)} \end{pmatrix}$$

The PONS waveforms form a matrix of size $2^N \times 2^N$, N being any positive number, where each row has a mating row that constitutes a complementary pair. The symmetric PONS construction starts from any pair of complementary sequences p_1 and p_2, of length L and obtains four vectors 2L as

$$P^{(1)} = \begin{pmatrix} p_1 & p_2 \\ p_1 & -p_2 \\ p_2 & p_1 \\ -p_2 & p_1 \end{pmatrix}$$

To produce PONS matrix of size 2^N x 2^N begin with the first matrix which are now referred as $P^{(1)}$ and recursively apply them to $P_{2m-1}^{(k-1)}$,$P_{2m}^{(k-1)}$ of adjacent rows of the (k-1)th PONS matrix to form $2^k x 2^k$ matrix. Thus the 4x4 matrix formed by substituting the first row of $P^{(1)}$ for p_1 and the second row for p_2 in above equation we obtain

$$P^{(2)} = \begin{pmatrix} 1 & 1 & 1 & -1 \\ 1 & 1 & -1 & 1 \\ 1 & -1 & 1 & 1 \\ -1 & 1 & 1 & 1 \end{pmatrix}$$

Similarly the next PONS matrix of size 8x8, is formed by applying (1) using the first two rows of the matrix $P^{(2)}$ to generate the first 4 rows of the matrix $P^{(3)}$ and last two rows of $P^{(2)}$ to generate the last 4 rows of $P^{(3)}$.

2.3.4.3 Performance improvement of OTDR using CCPONS

The PONS code constructed is a bipolar code. For application in OTDR it has to be converted to a unipolar code. The theoretical code gain of PONS was found [5] to be

$$\text{Codegain} = \sqrt{\frac{L}{2}} \qquad (2.24)$$

where L is the length of code.

It has been found through experiments that for a codeword of length L=64, the code gain of CCPONS, biorthogonal and simplex code are 3.76, 3.0442 and 3.0274 dB. The PAPR of PONS has been found to be 2 through experiments.

Figure below shows us the code gain obtained while using CCPONS

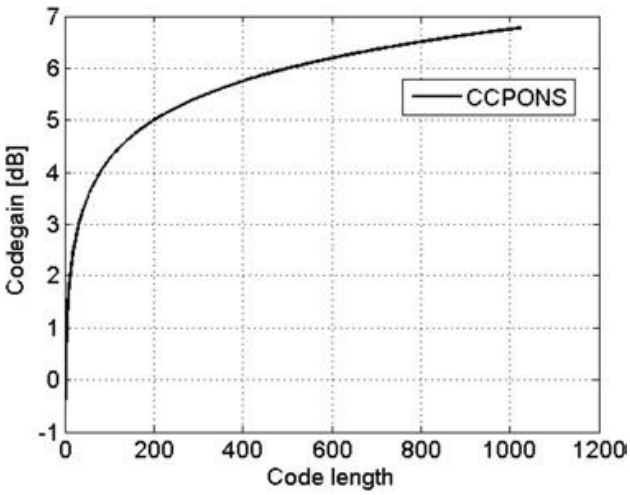

Fig. 2.4: Code gain variation of CCPONS.[5]

2.4 Conclusion:

In this chapter we saw how the application of the codes instead of a single pulse helps in increasing the coding gain of the OTDR without comprising the dynamic range. The code gain of each code is different and it affects an OTDR system in a different manner. Also what is most important in the case of these codes is the PAPR value that determines efficiency of the code. Figure 2.5 gives us a comparative idea of how the code gains of these codes vary with code length.

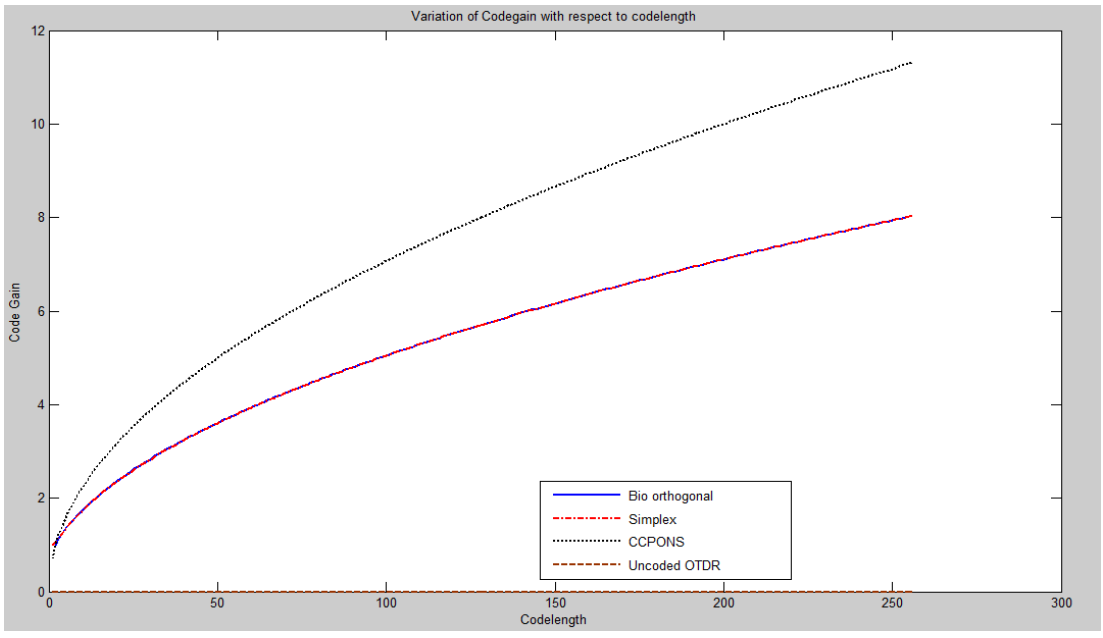

Fig. 2.5: Comparison of Code gain for different code length of different codes.

CHAPTER 3

EXPERIMENTS USING CONVENTIONAL OTDR

3.1 **Experimental Studies on an OTDR:**

The experimental studies were performed on an Agilent 6000 series OTDR at IIT Kharagpur. The details are as follows.

3.1.1 Objective of the experiment:

To understand the workings of an OTDR and to take real-time measurements from single mode and multi mode fibres using the OTDR

3.1.2 Equipment:

1. Agilent E6003A mini-OTDR
2. Optical fibre, singlemode fibre of 500 metres length and two multimode fibres of lengths 1000 metres and 500 metres.
3. Mechanical connectors

3.1.3 Experimental setup

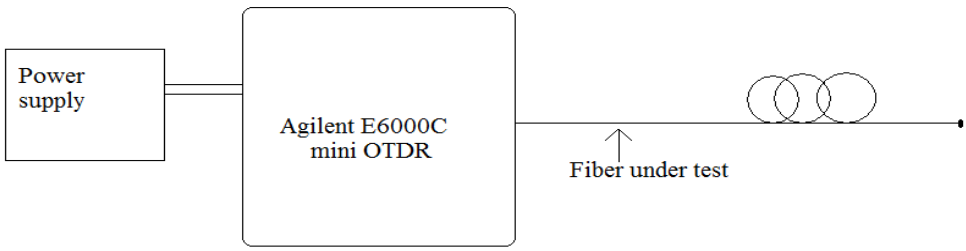

Fig 3.1: Experimental setup used to perform the experiment.

3.1.4 OTDR specifications:

The Agilent E6003A mini-OTDR comes equipped with an exhaustive user manual. Due to the fragility of the OTDR equipment, it was vital that the instructions in the manual were accurately followed. The manual also held specifications for the instrument. Specifications are as follows,

Laser Type	FP – InGaAsP
Laser class	3A/Class 1 (Europe/US
std) O/P power (pulse max)	50 mW

Pulse duration	10µs (max)
O/P power (CW)	500µW
Beam waist diameter	9µm
Numerical Aperture	0.1
Wavelength	1310/1550 ± 25 nm
Observations:	
Refractive index of fiber: 1.471	Pulse width setting:10 ns

3.1.5 Observations:

3.1.5.1 Case 1:

Single mode fiber

OTDR wavelength setting 1310 ±25 nm

End to end length as per OTDR trace: 506.28 m

Front end reflection: -10.60 dB

Rear end reflection: -13.60 dB

2-point attenuation: 54.977 dB/Km

2-point loss: 27.834 dB

Range setting of OTDR: 0-1 Km

Optical return loss: 10.59 dB/Km

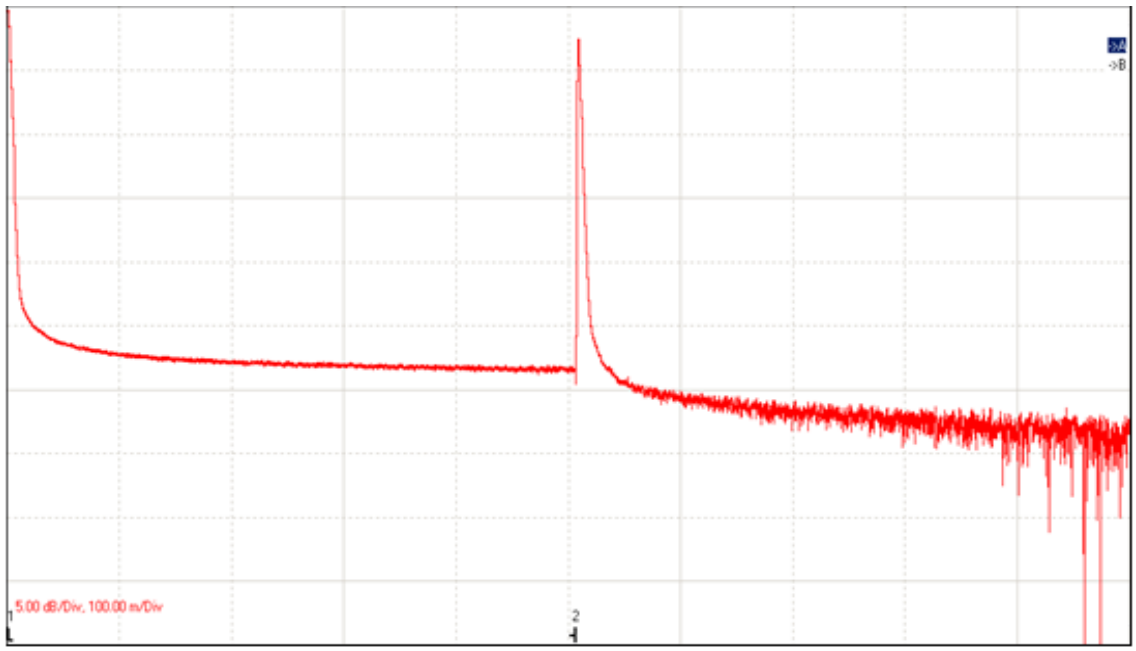

Fig 3.2: OTDR trace of SMF at 1310 nm wavelength

The above trace was obtained on the mini-OTDR monitor during the course of the experiment using a singlemode fiber at 1310 nm wavelength.

3.1.5.2 Case 2:

Single mode fiber

OTDR wavelength setting 1550 ±25 nm

End to end length as per OTDR trace: 506.28 m

Front end reflection: -10.60 dB

Rear end reflection: -14.40 dB

2-point attenuation: 59.577 dB/Km

2-point loss: 30.163 dB

Refractive index of fiber: 1.471

Range setting of OTDR: 0-1 Km

Optical return loss: 10.37 dB/Km

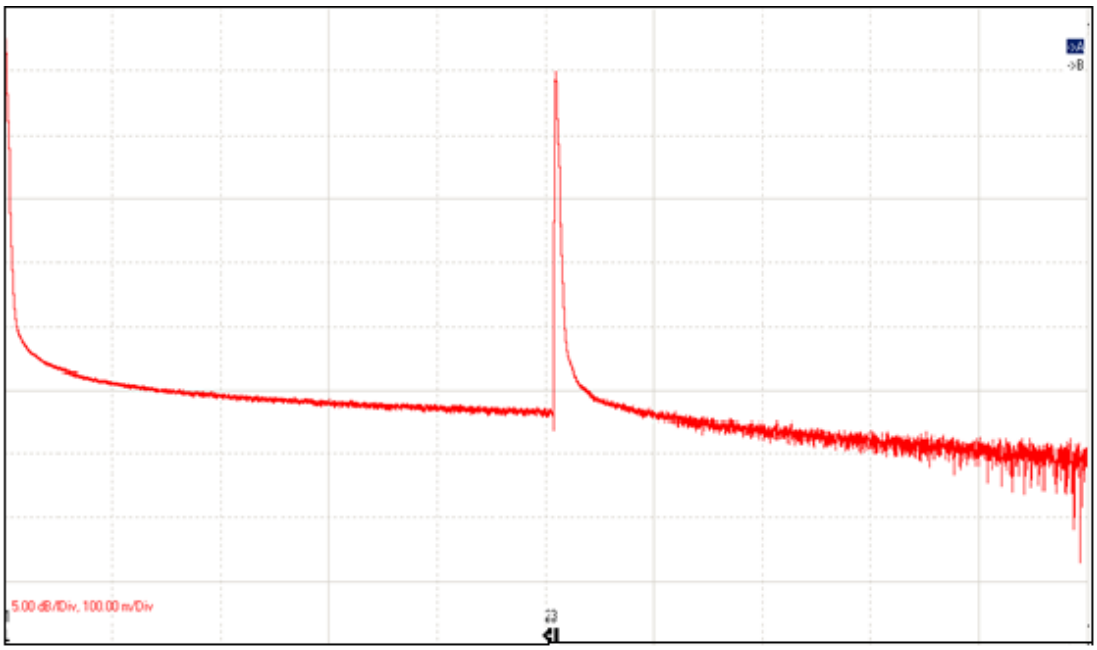

Fig 3.3: OTDR trace of SMF at 1550 nm wavelength

The above trace was obtained on the mini-OTDR monitor during the course of the experiment using a singlemode fiber at 1550 nm wavelength.

3.1.5.3 Case 3:

Multi mode fiber

OTDR wavelength setting 1310 ±25 nm

End to end length as per OTDR trace:

1st fiber: 510.11 m

2nd fiber: 1503.23 m

Front end reflection: -10.60 dB

Rear end reflection: -14.40 dB

2-point attenuation: 16.193 dB/Km

2-point loss: 24.565 dB

Range setting of OTDR: 0-2 Km

Optical return loss: 14.11 dB/Km

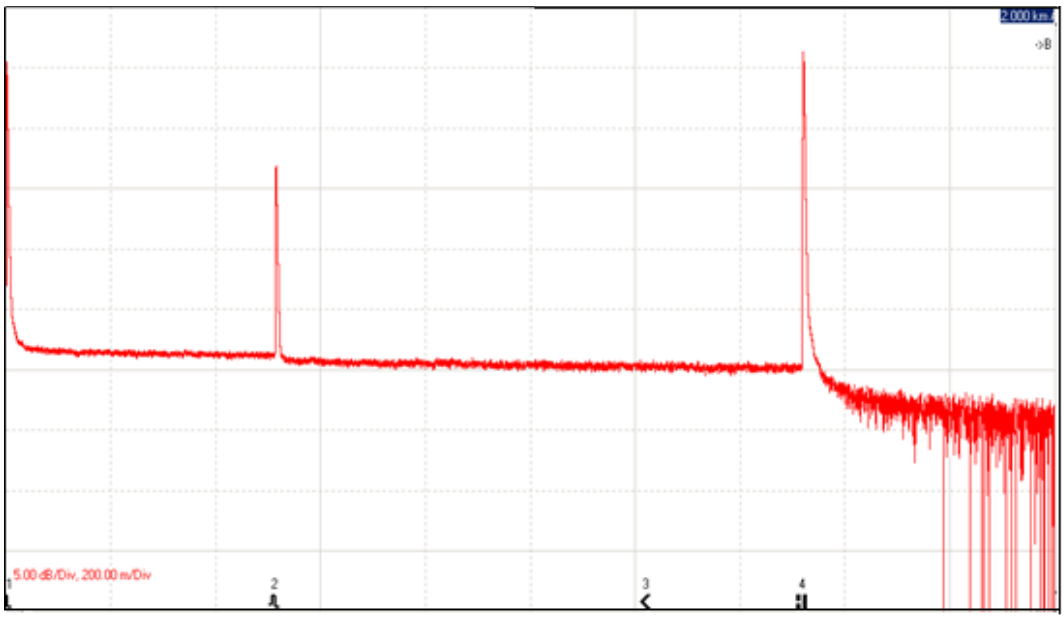

Fig 3.4: OTDR trace of MMF at 1310 nm wavelength

The above trace was obtained on the mini-OTDR monitor during the course of the experiment using a multimode fiber at 1310 nm wavelength.

3.1.5.4 Case 4:

Multi mode fiber

OTDR wavelength setting 1510 ±25 nm

End to end length as per OTDR trace:

1st fiber: 510.11 m

2nd fiber: 1503.23 m

Front end reflection: -10.60 dB

Rear end reflection: -12.56 dB

Reflection at connector: -45.67 dB

2-point attenuation: 20.722 dB/Km

2-point loss: 31.350 dB

Range setting of OTDR: 0-2 Km

Optical return loss: 10.59 dB/Km

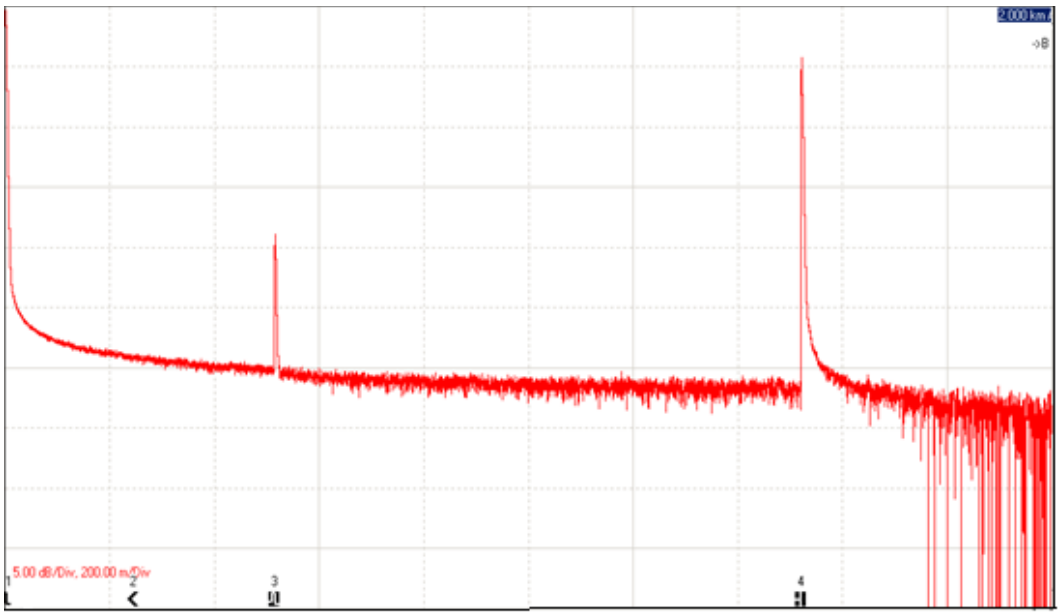

Fig 3.5: OTDR trace of MMF at 1550 nm wavelength

The above trace was obtained on the mini-OTDR monitor during the course of the experiment using a multimode fiber at 1550 nm wavelength.

3.2 Conclusion:

This chapter deals with the experiment involving a conventional OTDR and the traces observed on the OTDR screen are found to be matching with the theoretically predicted values.

CHAPTER 4

RESULTS AND FUTURE SCOPE OF WORK

4.1 Results:

The following table shows the code gains and associated PAPR values of the different codes we have dealt with in the previous chapters.

Coding technique	**Code Gain for a code length of 64**	**PAPR**
Golay Code	3.01 db	4
Simplex Code	4.06 dB	≤2
Bi-Orthogonal Code	4.00 dB	2
Complementary Correlated Prometheus Ortho-Normal Sequence	5.66 dB	2

Table 4.1: Coding gains and PAPRs of the codes concerned.

From this data and the experimental results obtained from the experiment performed at IIT Kharagpur using a conventional OTDR, we are able to draw some important conclusions.

PAPR technically gives us information about the amount of power that is sent in the signal. Remember that the signal sent is not sinusoidal but rather a series of pulses modulated according to an unipolar coding sequence. Low PAPR is essentially the requirement for all systems involving digital communication and the above coding techniques seem to help reduce PAPR. PAPR can increase in conventional OTDR because sometimes the pulse may spike causing the maximum power to become much larger than the average power of the pulse causing PAPR to increase. Also unipolar coding has the advantage over standard coding and modulating techniques as in unipolar coding, the average signal power is always greater than zero, where as in standard modulating techniques the carrier signal used is sinusoidal and the average signal power is zero in such cases causing infinite PAPR. From the coding techniques discussed, PAPR of CCPONS and Simplex is found to be the lowest and hence most suited for the required applications.

4.2 Advantages of Coding over Conventional OTDR:

The basic principle in OTDR is to send a small signal through an optical fibre and observe the reflected light. The intensity of the reflected light depends upon many parameters like nature of the fibre, wavelength of light etc. One of the parameters influencing this is the power of the input signal. Larger the input power, larger will be the distance it covers within the fibre. The easiest way of increasing input power would be to send n number of pulses one after the other. But this method has a drawback because u cannot just send pulses like that as it will result in the receiver getting saturated very quickly and it will result in a permanent dead zone that renders the analysis ineffective.

This is where the concept of coding shows its advantage. By using unipolar coding techniques, one is able to send a large amount of input power by using less number of pulses. This way we are able to avoid the scenario of receiver getting saturated.

The other advantages of coding techniques over conventional OTDR include better dynamic range and greater spatial resolution with a definite amount of noise present in the system.

4.3 Future scope and prospects:

Throughout this thesis, we have been discussing the different parameters of an OTDR and how external factors can affect them. In the different chapters we have seen how coding is one of the ways to improve the SNR of an OTDR system and also through different coding methods a better dynamic range and spatial resolution trade off can be achieved.

The experiment performed using the Agilent Mini-OTDR at IIT Kharagpur helped us understand the tracing phenomenon of the OTDR. It is crucial to understand the fact each OTDR manufacturer chooses the different characteristics to be included in their OTDR design. The feature not so commonly found though is the ability to integrate a PC based OTDR into a single kit. Most practical experiments involving the testing of coding revolves around a circuit that is similar to the one shown below.

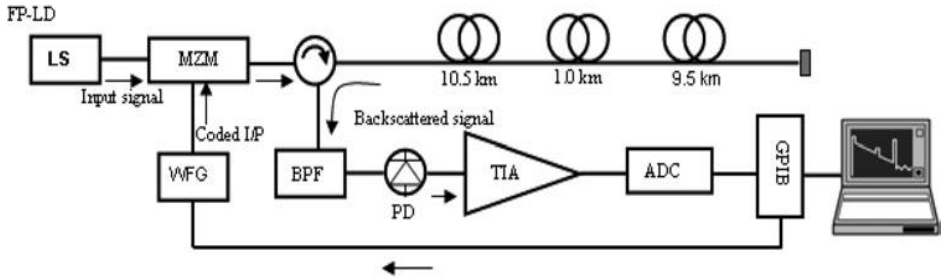

Fig 4.1: The excessive equipment required to integrate coding into an OTDR.[5]

This figure is the experimental setup that was used to implement CCPONS code in an OTDR. The entire circuitry except for the waveform generator (WFG) and the modulator (MZM) is integrated into the current available models of OTDR. The waveform generator and the modulator are the two components of this setup that allow the CCPONS code to be integrated in the testing mechanism.

Throughout the years, the process of implementing various codes and sequences in an OTDR has involved extensive setups like the ones above. But the results of the implementing these codes has been obvious each time a new code is developed. The results of the various experiments performed can be used to facilitate research into design of new OTDR machines which implement these coding techniques in their probing mechanisms. This will result in better fault analysis and the ability of the OTDR to analyze extremely long fibres.

The different experiments and its results that have been studied in this thesis can be used in future to design highly efficient OTDR systems that will be able to provide a better SNR, lower PAPR and in affect improve the dynamic range of the OTDR to a far greater degree.

4.4 Conclusion:

From this chapter it can be concluded that OTDR systems implementing various unipolar codes out perform a conventional OTDR system and by implementation of such codes, PAPR of the signal can be reduced that helps to add to the efficiency of the OTDR system

REFERENCES:

[1] Jozef Jasenek, Iozefa Cervenova, Marek Hlavac , "The enhancement of signal to noise in OTDR by the use of probe signal coding." IEEE Bratislava, May 2001, vol. 3, pp. 47–51

[2] Duckey Lee, Hosung Yoon, Na Young Kim, and Namkyoo Park, "SNR Improvement of a Non-Coherent OTDR Using Biorthogonal Codes and Moore-Penrose Generalized Inverses." ECOC 2004 Proceedings-Vol.3 Paper We4.P.156

[3] Duckey Lee,Hosung Yoon,Pilhan Kim,Jonghan Park,and Namkyoo Park, "Optimization of SNR Improvement in the Noncoherent OTDR Based on Simplex Codes." Journal of Lightwave technology,Vol 24,No.1,January 2006

[4] Michael D.Jones, "Using simplex code to improve OTDR sensitivity." IEEE phototonics technology letters,VOL 15,No.7,July 1993

[5] P.K.Sahu,S.C.Gowre,S.Mahapatra,"Optical time-domain reflectometer performance performance improvement using complementary correlated Prometheus Orthonormal Sequence"IET Optoelectronics 2007

[6] M.Nazarathy and group, "Real time long range complementary correlation optical time domain reflectometer", J. Light Wave technol., Vol. 7, pp. 24-38, Jan. 1989

[7] BETHEA C.G., LEVINE B.F., CAVA S., RIPAMONTI G.: 'Highresolution and high-sensitivity optical-time-domain reflectometer', Opt. Lett., 1988, 13, Vol 3, pp. 233–235

[8] HEALEY P., MALYON D.J.: 'OTDR in single-mode fiber at 1.5 mm using heterodyne detection', Electron. Lett., 1982, 18, vol 12, pp. 862–863

[9] BARFUSS H., BRINKMEYER E.: 'Modified optical frequency domain reflectometry with high spatial resolution for components of integrated optic systems', J. Lightwave Technol., 1989, 7, vol 1, pp. 3–10

[10] TATEDA M., HORIGUCHI T.: 'Advances in optical time-domain reflectometry', J. Lightwave Technol., 1989, 7, vol 8, pp. 1217–1224

[11] GILGEN H.H., NOVAK R.P., SALATHE R.P., HODELW.: 'Submillimeter optical reflectometry', J. Lightwave Technol., 1989, 7, vol 8, pp. 1225–1233

[12] KAPRON F.P., ADAMS B.P., THOMAS E.A., PETERS J.W.: 'Fiber-optic reflection measurements using OCWR and OTDR techniques', J. Lightwave Technol., 1989, 7,vol 8, pp. 1234–1241

[13] NAZARATHY M., NEWTON S.A., GIFFORD R.P., MOBERLY D.S. SISCHKA F., TUNTA W.R., FOSTER S.: 'Real-time long range complementary correlation optical time domain reflectometer', J. Lightwave Technol., 1989, 7,vol 1, pp. 24–38

[14] KOYAMADA Y., NAKAMOTO H.: 'High performance single mode OTDR using coherent detection and fiber amplifiers', Electron. Lett., 1990, 26,vol 9, pp. 573–575

[15] KIM P., YOON H., SEO J, ET AL.: 'Novel in-service supervisory system using OTDR for long-haul WDM transmission link including cascaded in-line EDFAs', IEEE Photonics Technol. Lett., 2001, 13, vol 10, pp. 1136–1138

[16] DE MATOS C.J.S., TAYLOR J.R.: 'Optical time-domain reflectometry of discrete fiber Raman amplifiers', IEEE Photonics Technol. Lett., 2003, 15, vol 8, pp. 1064–1066

[17] LEE D., YOON H., KIM P., PARK J., KIM NA.Y., PARK N.: 'SNR enhancement of OTDR using biorthogonal codes and generalized inverses', IEEE Photonics Technol. Lett., 2005, 17, vol 1, pp. 163–165

[18] DE MULDER B., CHEN W., BAUWELINCK J., VANDEWGE J., QIU X.-Z.: 'Nonintrusive fiber monitoring of TDM optical networks', J. Lightwave Technol., 2007, 25, vol 1, pp. 305–317

[19] LEE D., YOON H., KIM NAY., LEE H., PARK N.: 'Analysis and experimental demonstration of simplex coding technique for SNR enhancement of OTDR'. IEEE LTIMC Proc., New York, USA, October 2004, pp. 118–122 [20] POPOVIC B.M.: 'Spreading sequences for multicarriers CDMA systems', IEEE Trans. Commun., 1999, 47, vol 6, pp. 918–926

[21] BYRNES J.S., SAFFARI B., SHAPIRO H.S.: 'Energy spreading and data compression using the Prometheus orthonormal set'. IEEE, Digital signal Processing Workshop Proc., Norway, September 1996, pp. 9–12

[22] ZULCH P., WICKS M., MORAN B., SUVOROVA S., BYRNES J.: 'A new complementary waveform techniques for radar signals'. IEEE Radar Conf. Proc., California, April 2002, pp. 35–40

[23] DELIC H., BYRNES J.S., OSTHEIMER G.: 'The Prometheus orthonormal set for wideband CDMA'. Proc. IEEE MELECON, Croatia, May 2004, vol. 2, pp. 437–440

[24] K. Okada and K. Hashimoto, "Optical cable fault location using correlation technique," *Electron. Lett.*, vol. 16, pp. 629–630, 1980.

[25] P. Healey, "Optical orthogonal pulse compression codes by hopping," *Electron. Lett.*, vol. 17, pp. 970–971, 1981.

[26] M. Nazarathy, S. A. Newton, R. P. Giffard, D. S. Moberly, F. Sischka, W. R. Trutna Jr., and S. Foster, "Real-time long range complementary correlation optical time domain reflectometer," *J. Lightw. Technol.*, vol. 7, pp. 24–38, Jan. 1989.

[27] M. Jones, "Using simplex codes to improve OTDR sensitivity," *IEEE Photon. Technol. Lett.* July 1993, vol. 15, pp. 822–824.

[28] Y. Gong and A. D. Stokes, "Resolution of correlation optical time domain reflectometry," in *CLEO/PACIFIC RIM*, 1995, Paper P97, pp. 303–304.

[29] B. Sklar, *Digital Communications*. Englewood Cliffs, NJ: Prentice- Hall, 1988.

[30] S. L. Campbell and C. D. Meyer Jr., *Generalized Inverses of Linear Transformations*. New York: Pitman, 1979.

[31] J. A. Decker, Jr., "Experimental realization of the multiplex advantage with a Hadamard-transform spectrometer," *Appl. Opt.*, Mar. 1971. vol. 10, no. 3, pp. 510–514.

[32] M. Harwit and N. J. Sloane, *Hadamard Transform Optics*. New York: Academic, 1979.

[33] E. E. Fenimore and G. S. Weston, "Fast delta Hadamard transform," *Appl. Opt.* Sep. 1981, vol. 20, no. 17, pp. 3058–3067.

[34] A. S. Sudbo, "An optical time-domain reflectometer with low-power InGaAsP diode lasers," *J. Lightw. Technol.* Dec. 1983, vol. LT-1, no. 4, pp. 616–618,

[35] James A. Davis and Jonathan Jedwab, "Peak-to-Mean Power Control in OFDM, Golay Complementary Sequences, and Reed-Muller Codes," IEEE Transactions on information theory,

Nov 1999 Vol. 45, No 7, pp. 2397-2417,

[36] Kenneth G. Paterson and Vahid Tarokh, "On the Existence and Construction of Good Codes with Low Peak-to-Average power Ratios," IEEE Transactions on information theory, Sept 2000 Vol. 46, No 6, pp. 1974-1987.

[37] Rudolf Lidl, Harald Niederreiter and P. M. Cohn, Finite Fields, Cambridge University Press, Cambridge, 1997.

[38] F. J. Macwilliams and N. J. A. Sloane The theory of Error-correcting Codes, Amsterdam, The Netherlands: North-Holland, 1986.

[39] Sethuraman, B. A.; Rajan, B. S.; Shashidhar, V. "Full-diversity, high-rate space-time block codes from division algebras," IEEE Transactions on information theory: Special Issue on Space-Time Transmission, Reception, Coding and Signal Design, Oct. 2003, Volume 49, no. 10, pp. 2596 - 2616.

[40] Prabal Paul, C. R. Pradeep and B. Sundar Rajan, "On the PAPR of cosets of linear codes," manuscript.

[41] Shashidhar, V. "High-Rate and Information-Lossless Space-Time Block Codes from Crossed-Product Algebras," Ph-d thesis, Department of E. C. E., IISc, April 2004.

[42] Oggier Fr´ed´erique, Viterbo Emanuele, "Algebraic Number Theory and Code Design for Rayleigh Fading Channels, ", now Publishers Inc. 2004.

[43] Md. Zafar Ali Khan, "Single-symbol and Double-symbol Decodable STBCs for MIMO Fading Channels," Ph-d thesis, Department of E. C. E., IISc, January 2005.

[44] Belfiore J. C., Rekaya G. and Viterbo E., "The Golden Code: A 2 × 2 Full-Rate Space- Time Code With Nonvanishing Determinants," Proceedings of the IEEE International Symposium on Information Theory, 2004.

[45] Technical note-194, EXFO OTDR manual released with EXFO OTDR products.

[46] P. **S.** Moharir and A. Selvarajan, "Optical Barker codes," *Electron. Lett.,* 1974, vol. 10, pp. 154-155,

[47] M. Nazarathy, **S.** A. Newton, and W. R. Trutna, "Complementary correlation OTDR with three codewords," *Electron. Lett.* 1990, vol. *26,* pp. 70-71.

[48] J. Cheng, J. H. Goll, and N. Edwards, "Method and apparatus for carrying out fiber optic time domain reflectometry wherein Golay complementary sequences are applied," US. May 1988, Patent no: 4 743 753.

[49] S. Wright, R. E. Epworth, D. F. Smith, and J. P. King, "Practical coherent OTDR at 1.3 microns," in *Proc. 2nd Opt. Fiber Sensors Con$,* Stuttgart, West Germany, 1984, pp. 347-350.

[50] P. Henlely, R. C. Booth, B. E. Daymond-John, and B. K. Nayar, "OTDR in single-mode fibre at 1.5 Fm using homodyne detection," *Electron. Lett* 1984., vol. *20,* pp. 360-362.

[51] M. Hanvit and N. J. A. Sloane, *Hadamard Transfom Optics* 1979. London: Academic.

[52] Kenneth G. Paterson and Vahid Tarokh, "On the Existence and Construction of Good Codes with Low Peak-to- Average Power Ratios", ISlT *2000,* June 25-30,2000, Sorrento, Italy.